

Molecular Physics

An International Journal at the Interface Between Chemistry and Physics

ISSN: (Print) (Online) Journal homepage: www.tandfonline.com/journals/tmph20

Manifestation of the normal intensity distribution law (NIDL) in the rovibrational emission spectrum of hydroxyl radical

Emile S. Medvedev, Aleksander Yu. Ermilov & Vladimir G. Ushakov

To cite this article: Emile S. Medvedev, Aleksander Yu. Ermilov & Vladimir G. Ushakov (26 Aug 2024): Manifestation of the normal intensity distribution law (NIDL) in the rovibrational emission spectrum of hydroxyl radical, *Molecular Physics*, DOI: [10.1080/00268976.2024.2395439](https://doi.org/10.1080/00268976.2024.2395439)

To link to this article: <https://doi.org/10.1080/00268976.2024.2395439>

 View supplementary material 

 Published online: 26 Aug 2024.

 Submit your article to this journal 

 View related articles 

 View Crossmark data 

Manifestation of the normal intensity distribution law (NIDL) in the rovibrational emission spectrum of hydroxyl radical

Emile S. Medvedev ^a, Aleksander Yu. Ermilov ^b and Vladimir G. Ushakov ^a

^aFederal Research Center of Problems of Chemical Physics and Medicinal Chemistry (former Institute of Problems of Chemical Physics), Russian Academy of Sciences, Chernogolovka, Russian Federation; ^bM. V. Lomonosov Moscow State University, Moscow, Russian Federation

ABSTRACT

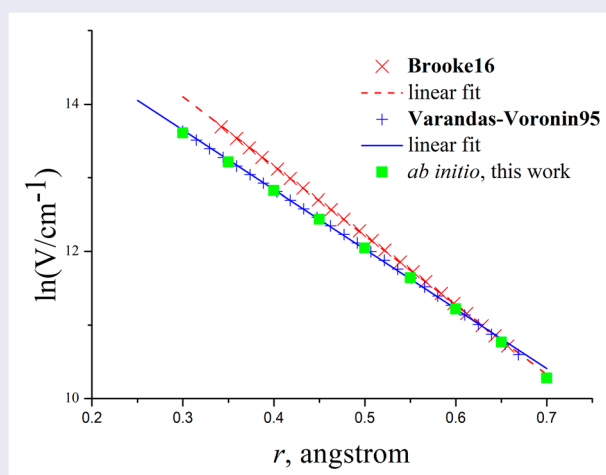
The latest experimental [Noll *et al.* Atmos. Chem. Phys. **20**, 5269 (2020)] and theoretical [Brooke *et al.* J. Quant. Spectr. Rad. Transfer **168**, 142 (2016)] data on the OH emission intensities are analysed with use of the NIDL. It is found that the calculated intensities of the $\Delta v > 6$ transitions should not be trusted. The analysis of the OH data revealed that the NIDL theory is not applicable to the satellite bands. The effect of small reduced mass previously discovered in H₂ [Ushakov *et al.* J. Mol. Spectrosc. **399**, 111863 (2024)], causing the NIDL straight-line slope to be larger than the one associated with the repulsive branch of the potential, is demonstrated in OH, and the same should be true of all the diatomic hydrides. We performed *ab initio* calculations of the OH repulsive branch and compared it with the one of Brooke *et al.* and the other due to Varandas and Voronin [Chem. Phys. **194**, 91 (1995)]. We found that the *ab initio* PEF closely follows the Varandas-Voronin potential in the repulsive region important for calculating the overtone intensities [Medvedev, J. Chem. Phys. **137**, 174307 (2012)].

ARTICLE HISTORY

Received 13 March 2024
Accepted 14 August 2024

KEYWORDS

Overtone transitions;
repulsive branch; *ab initio* calculations



1. Introduction

More than 30 years ago, two of us in collaboration with our beautiful friend and colleague Aleksander Nemukhin published paper [1] in support of the NIDL theory (see review [2] and references therein). The theory has been verified by the available experimental and theoretical data for a number of diatomic molecules and quasi-diatom local vibrations in polyatomic molecules, and it has proven to be a powerful tool to control the precision of the calculated intensities of the overtone transitions [3,

4]. In particular, the OH observational data of Krassovsky *et al.* [5] and Cosby and Slanger [6] were used to demonstrate the NIDL behaviour of the relative emission intensities [2, 7].

In this paper, we use the contemporary data on hydroxyl radical [8–10] to verify the NIDL for emission and to demonstrate the utility of the NIDL for the analysis of the calculated overtone intensities.

We perform the *ab initio* calculations of the PEF repulsive branch important for calculations of the overtone

CONTACT Emile S. Medvedev  medvedev@icp.ac.ru  Federal Research Center of Problems of Chemical Physics and Medicinal Chemistry (former Institute of Problems of Chemical Physics), Russian Academy of Sciences, 1 Prospekt Akademika N. N. Semenova, Chernogolovka 142432, Russian Federation
Supplemental data for this article can be accessed online at  <http://dx.doi.org/10.1080/00268976.2024.2395439>.

intensities [2]. The calculated repulsive branch is compared with the ones of two literature PEFs to determine which one is more suited for calculations of the overtone intensities.

Section 2 gives a brief review of the predictions of the NIDL theory for emission. Sections 3 and 4 provide for verifications of these predictions in the emission spectra. Section 5 describes the *ab initio* calculations and their significance for the calculations of the overtone intensities. Section 6 summarises our findings. Section 7 provides for additional considerations.

2. Predictions of the NIDL theory

The NIDL theory is based on the quasi-classical approximation, which states that, at high-enough energies, the vibrational wave function can be represented in the form $p^{-1/2} \exp(iS/\hbar)$, where p and S are classical momentum and action in a given vibrational state, E_ν , which is formally equivalent to $\nu \gg 1$. In practice, however, $\nu \geq 2$ is sufficient.¹

Another important feature of the theory is application of the Franck-Condon principle, which states that, due to a large difference between the electron and nuclear masses, any optical transition at frequency ν between states 1 and 2 occurs at a fixed nuclear configuration, r^* , where the nuclear momenta coincide, $p_1(r^*) = p_2(r^*)$, and the potentials differ by the photon energy, $U_1(r^*) = U_2(r^*) + h\nu$.

In application to the rovibrational transitions within the ground electronic state, where $U_1(r) = U_2(r) \equiv U(r)$, the Franck-Condon principle means [11, Sections 5.4–5.6] that the main contribution to the transition-dipole-moment (TDM) integral is provided by a vicinity of point r^* in the complex plane where the potential-energy function (PEF) has singularity, $U(r) \rightarrow \infty$, see §51 in Ref. [12].

There is one and only one *physical* singularity of $U(r)$, namely that at $r = 0$, due to the Coulomb nuclear repulsion,² therefore the repulsive branch of $U(r)$ plays a crucial role in determining the overtone intensities. If we approximate the repulsive branch with a simple exponential function, $U(r) \propto \exp(-2\beta r)$, then the TDM squared³ for the overtone transition ($\Delta\nu \equiv \nu' - \nu'' \geq 2$) from the upper level ν' to the lower level ν'' obeys the NIDL,

$$\log \text{TDM}_{\nu'\nu''}^2 = \text{const} - a\sqrt{E_{\nu'}/\omega}, \quad (1)$$

where the energy and harmonic frequency of vibration, ω , are in cm^{-1} , and the upper level is assumed to be high, $\nu' \geq 2$, which occurs in both absorption and emission. The const is assumed to be a slow function of ν' at a given

ν'' ⁴ except for the anomalies [2, Section II], which do not obey the NIDL and must be excluded from the data fitting.

If the lower level is also high, $\nu'' \geq 2$, which is often met in emission, then the NIDL for the ratio of the intensities, TDM^2 , for two overtone transitions starting at a common upper level takes the form (we omit primes for brevity)

$$\log \left(\frac{\text{TDM}_{\nu\nu_1}}{\text{TDM}_{\nu\nu_2}} \right)^2 = a \left(\sqrt{\frac{E_{\nu_1}}{\omega}} - \sqrt{\frac{E_{\nu_2}}{\omega}} \right),$$

$$\nu_1 > \nu_2 \geq 2, \quad \nu - \nu_1 \geq 2, \quad (2)$$

where a is the same as in Equation (1). Here, the const disappears because the left-hand side vanishes at $\nu_1 = \nu_2$. In fact, due to approximate nature of the NIDL, there is a small const, on the order of the statistical error, which, however, becomes large at the anomalies; yet, the anomalies are ignored in the NIDL plots.

Finally, if the lowest level is 0 or 1, then Equation (2) is modified as follows:

$$\log \left(\frac{\text{TDM}_{\nu\nu_1}}{\text{TDM}_{\nu\nu_2}} \right)^2 = \text{const} + a\sqrt{\frac{E_{\nu_1}}{\omega}}, \quad \nu_2 = 0, 1 \quad (3)$$

(for more details, see review [2] and references therein).

Graphically, Equations (1)–(3) are represented, in the respective coordinates, by straight lines with slope a , which is connected to the steepness, β , of the repulsive branch of the PEF by relation [2]

$$a = \frac{\pi}{\beta r_e \ln 10} \sqrt{\frac{\omega}{B_e}}, \quad (4)$$

where r_e is equilibrium bond length, harmonic frequency ω and rotational constant B_e are in cm^{-1} .

There are several consequences of the above equations that are easy to verify. Equation (1) predicts the exponential decrease of the intensities with the overtone number, of which the pace, a , given by Equation (4) is inversely proportional to the steepness of the repulsive branch of the PEF: the steeper the PEF, the slower the decay. The decay rate in Equation (4) depends solely on the PEF, being independent of the dipole-moment function (DMF), which affects only the const.⁵

Equation (2) predicts that the ratio of the intensities of two lines emitted from a common upper level, ν , is the same for various ν . This important feature of the overtone transitions was first noted by Ferguson and Parkinson [13], who even considered a possibility to use the linear DMF ('the relative intensities in the high overtone sequences are likely to be similar to those for a linear dipole moment').

Equation (4) permits direct verification of the NIDL theory by calculating β with the *ab initio* methods and comparing it with the one derived from the NIDL slope.

Finally, Equation (4) predicts that the NIDL slope is proportional to $M^{1/4}$, where M is the reduced mass. Hence, the slope for the HX molecules will be essentially less than for the heavier ones.

Here, we will use the theoretical [8] and experimental [9] data to verify the NIDL and to derive the β values from the NIDL slopes; then we perform the *ab initio* calculations to compare the above β with the steepness of the repulsive branches of both the present *ab initio* PEF and the literature PEFs.

3. Verification of Equations (1)–(3)

When plotting the data in the NIDL coordinates according to Equation (1), we discovered that only the main-band (intra-multiplet, $\Delta F = 0$) transitions obey the NIDL. This is illustrated in Figure 1, where the upper and lower panels show examples of the intra- and inter-combination ($\Delta F \neq 0$, satellite) lines. The reason for this different behaviour is explained by the fact that the very existence of the satellite transitions is due to the rotational mixing of two X multiplet sub-states with different potentials. Moreover, severe cancelation of various contributions to the TDM for the satellite transitions takes place [14–16], hence this is a special case not covered by the NIDL theory. We remind that the anomalies also do not obey the NIDL, hence we have here a second reason for the NIDL to fail.

Table 1 shows the NIDL slopes for a few main-band low- J transitions.⁶ Previously [7], it was found that $\beta = 3.57 \pm 0.22 \text{ \AA}^{-1}$ from the NIDL slope, $a = 5.54 \pm 0.33$, derived from the OH data by Krassovsky *et al.* [5]; a similar result was obtained in Ref. [2] from the HITRAN 2008 data. It is seen from the table that the NIDL slopes are very close to the one cited above.

In Figure 1, the $\nu = 9$ point looks like an anomaly, but in fact it manifests the beginning of chaotic behaviour of the intensities (see Section 7 for further comments), which is also confirmed for the other lines shown in Table 1. Therefore, the intensities at $\nu > 8$ are highly unreliable.

Figure 2 shows the relative intensities of the lines emitted from a common upper level. In the upper panel (the main-band transitions), the NIDL is drawn by the least-squares fitting of Equation (2) to all data excluding some anomalies.⁷ The lower panel demonstrates the failure of the NIDL theory for the satellite transitions. Indeed, the intensity ratio must be relatively insensitive to the upper level, see Equation (2). In the figure, vertical sets of points are seen that correspond to transitions from

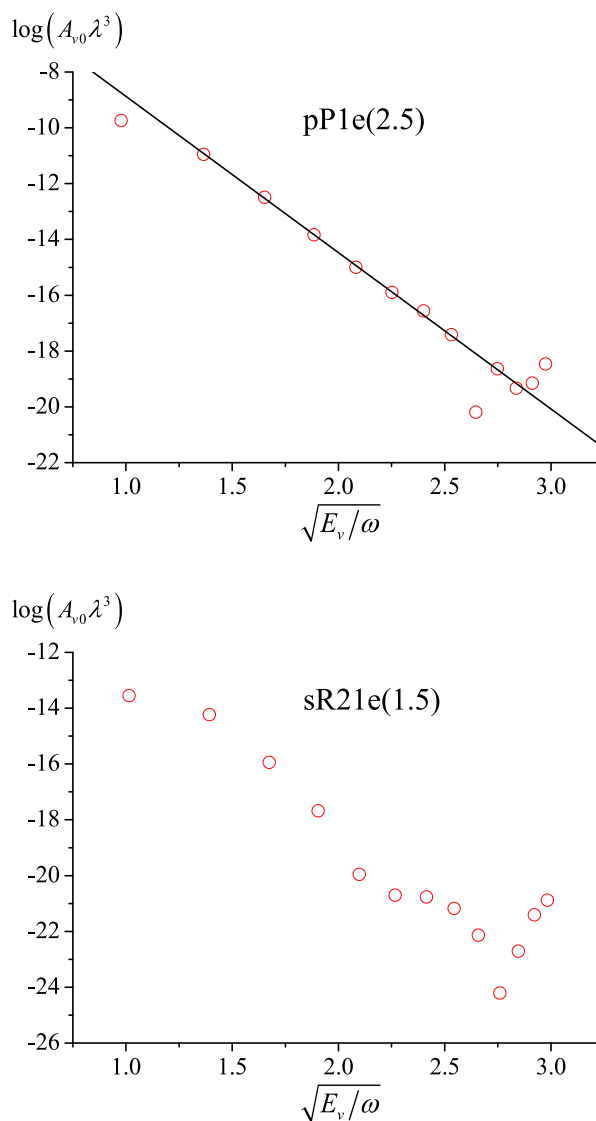


Figure 1. Einstein- A coefficients for the main-band low- J $\nu=0$ transitions, $\nu = 1-13$, from Ref. [8] normalised to the frequency factor to obtain TDM². The NIDL line in the upper panel is plotted by least-squares fitting of Equation (1) to the $\nu = 2-8$ intensities. Data at $\nu > 8$ are unreliable. The lower panel shows a wavy line, which testifies that the NIDL fails for the intercombination lines.

various upper levels, ν , to the same pair of the lower ones. Within each set, in contrast to the above prediction, the ratio varies dramatically, up to 5 orders of magnitude, which is comparable to the change of this ratio over the full range of abscissa (about 6 orders of magnitude); compare this with the upper panel where the variations within the vertical sets are much less, about 1.5 order of magnitude. The reason for failure the NIDL theory stems in the fact that the satellite lines are due to transitions between levels belonging to two different electronic states, whereas the NIDL is valid only for transitions within a single electronic state.

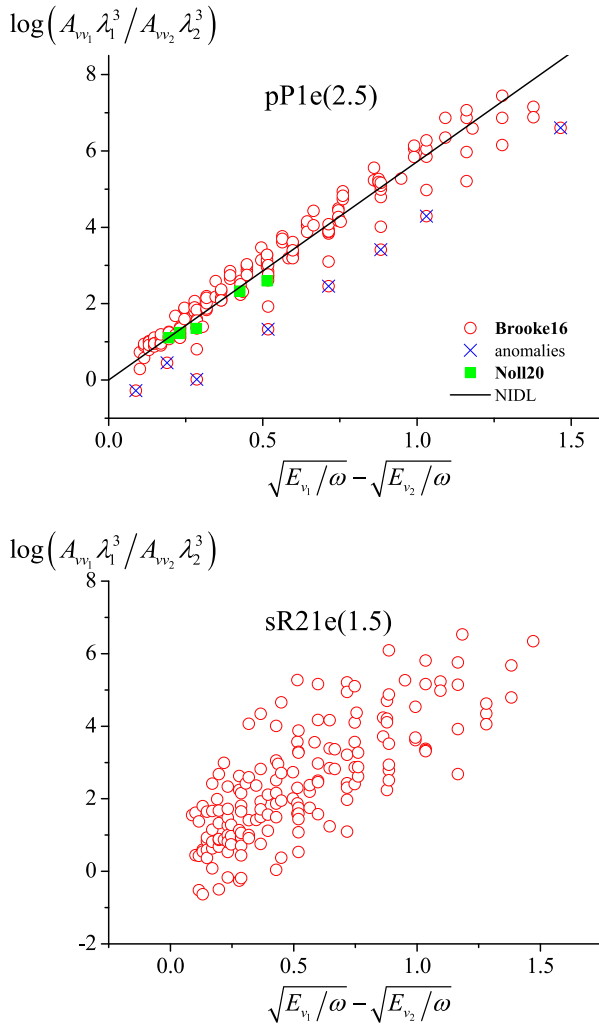


Figure 2. The relative intensities of the low- J $v - v_1$ and $v - v_2$ transitions from a common upper level v to lower levels $v_1 > v_2 \geq 2$, $v \geq v_1 + 2$. Circles, data from **Brooke16** [8]; crosses, the anomalies partly excluded⁷ from the NIDL plot of Equation (2); squares, the observational data from **Noll20** [9]. The upper panel shows the main-band transitions, the lower the satellite transitions not observed in **Noll20**; for the latter, the NIDL fails because the variations along the ordinate at a given abscissa are huge.

Table 2 presents the NIDL slopes of Equation (2) derived from the relative intensities of transitions with $v_2 \geq 2$ and v up to the maximum value of v_{\max} . The average value of the NIDL slope agrees with the one derived previously in Ref. [2] from the observational data of Krassovsky *et al.* [5] and of Cosby and Slanger [6].

Figure 3 shows an example of the NIDL plot according to Equation (3) for transitions involving the lowest level $v_2 = 1$. The NIDL slopes derived for some other low- J lines are collected in Table 3.

The data for transitions involving the lowest state $v_2 = 0$ are not shown as they contain too many anomalies that are not easy to exclude. The NIDL slope for this kind of transitions found in Ref. [7] is 5.62 ± 0.48 .

Table 1. The NIDL slopes derived from fitting the data of **Brooke16** [8] to Equation (1). The NIDL line is drawn across the $v = 2-8$ points.

Line	a
pP1e(2.5)	5.60 ± 0.10
pP2e(2.5)	5.59 ± 0.12
qQ1e(1.5)	5.61 ± 0.13
qQ2e(1.5)	5.84 ± 0.19
rR1e(2.5)	5.69 ± 0.17
rR2e(2.5)	5.74 ± 0.17
average	5.68 ± 0.15
Ref. [2]	$5.22 \pm 0.03^{a,b}$
	$5.77 \pm 0.02^{a,c}$

^aBased on the absorption data from HITRAN 2008. ^bFrom the plot of oscillator strength. ^cFrom the plot of oscillator strength divided by frequency.

Table 2. The NIDL slopes derived from fitting the data of **Brooke16** [8] to Equation (2).

Line	a	v_{\max}	No. ^a
pP1e(2.5)	5.72 ± 0.29	9	7
pP2e(2.5)	5.76 ± 0.28	9	5
qQ1e(1.5)	5.73 ± 0.29	9	7
qQ2e(1.5)	5.76 ± 0.29	9	7
rR1e(1.5)	5.76 ± 0.32	9	0
rR2e(1.5)	5.82 ± 0.33	9	0
rR1e(2.5)	5.81 ± 0.35	9	1
rR2e(2.5)	5.88 ± 0.38	9	7
average	5.78 ± 0.32		
Ref. [7]	5.54 ± 0.33		
Ref. [2]	5.36 ± 0.22		

^aThe number of the **Noll20** [9] experimental points in the plot.

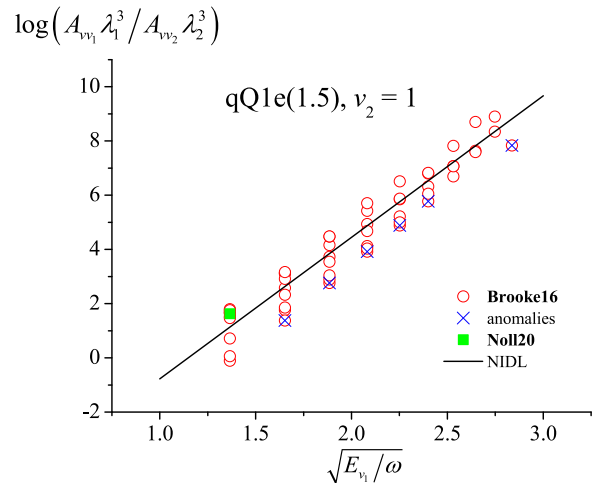


Figure 3. The same as in Figure 2 with $v_2 = 1$.

4. Verification of Equation (4)

Thus, we have got the NIDL slopes in the range of $5.22-5.88$, which results in the β values in the range of $(3.37-3.79) \text{ \AA}^{-1}$. Taking the largest statistical error of $\delta a = \pm 0.48$, we obtain $\delta \beta = (\beta/a)\delta a = \pm 0.35 \text{ \AA}^{-1}$. This results will be compared with the available data on the repulsive branch of PEF.

Table 3. The NIDL slopes derived from fitting the data of **Brooke16** [8] to Equation (3), $\nu_2 = 1$.

Line	a	ν_{\max}	No. ^a
pP1e(2.5)	5.18 ± 0.29	10	1
pP2e(2.5)	5.22 ± 0.28	10	1
qQ1e(1.5)	5.22 ± 0.29	10	1
qQ2e(1.5)	5.17 ± 0.29	10	1
rR1e(1.5)	5.23 ± 0.32	10	0
rR2e(1.5)	5.27 ± 0.33	10	0
rR1e(2.5)	5.25 ± 0.35	11	1
rR2e(2.5)	5.30 ± 0.38	10	1
average	5.22 ± 0.32		
Ref. [7]	5.88 ± 0.31		
Ref. [2]	5.34 ± 0.27		

^aThe number of the **Noll20** [9] experimental points in the plot.

The PEF of **Brooke16** is based on the RKR points and is presented in the tabular form in Supplementary material to Ref. [8]. One more PEF was developed by Varandas and Voronin in an analytic form [17]. The **Varandas-Voronin95** [17] potential was constructed so as to reproduce the asymptotic united- and separated-atoms limits. Figure 4 shows the repulsive branches of both these potentials. The boundaries of the repulsive branch are determined as follows: it must extend from the left turning point of the $\nu = 2$ level (0.67 \AA) down to a point r^* where the PEF reaches the value of $D_e(\nu_{\max}/2)^2$ where ν_{\max} is the desirable upper level [2]. Taking $\nu_{\max} = 10$, we obtain $r^* = 0.34 \text{ \AA}$ for the **Brooke16** PEF and 0.3 \AA for the **Varandas-Voronin95** PEF.

The β values obtained from the linear fits to both the PEFs are indicated in the figure caption, they are significantly larger than the above estimates. Inserting them into Equation (4), we obtain that the NIDLs associated with these two PEF's repulsive branches must have the slopes of $a = 4.19 \pm 0.01$ and 4.89 ± 0.02 , respectively, which are appreciably lower than those obtained from the NIDL plots shown in Tables 1–3. Thus we conclude that Equation (4) fails in the present case.

We have already encountered such a situation in molecular hydrogen [18], where it was found that the prefactor in the quasi-classical expression for the TDM is NOT a slow function of the vibrational quantum numbers, as was the case in CO [19] or PN [4]. It was shown that this is due to the small reduced mass of H_2 , which entails relatively small actions (on the order of 20 in the \hbar units) as compared to heavier molecules (~ 1500). OH also has a small mass, hence, the prefactor also contributes to the NIDL slope.

In summary, *in the H-containing diatomics, the NIDL slope derived from the calculated and/or observed intensities will always be larger than the one predicted from the steepness of the repulsive branch by Equation (4).*

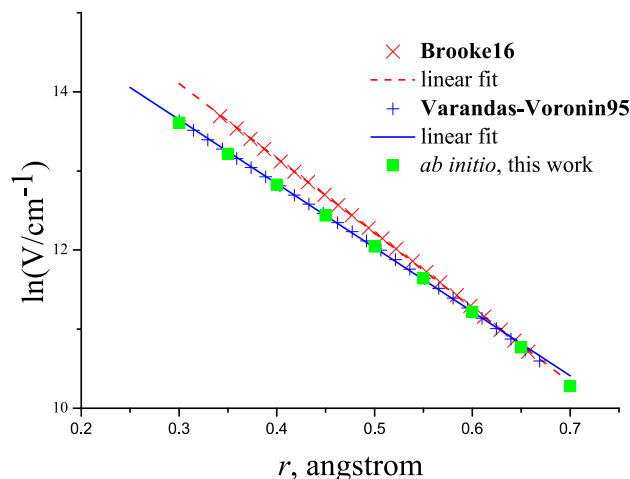


Figure 4. The repulsive branches of two PEFs with linear fits, which give $\beta = 4.72 \pm 0.01 \text{ \AA}^{-1}$ for the **Brooke16** [8] PEF and $4.05 \pm 0.02 \text{ \AA}^{-1}$ for the **Varandas-Voronin95** [17] PEF.

5. The *ab initio* calculations of the repulsive branch

In Figure 4, it is seen that the repulsive branches of the two PEFs are essentially different. Since the steepness of the repulsive branch affects the overtone intensities [2], it is interesting to learn which one of these PEFs has correct β .

To this end, we performed *ab initio* calculations of the PEFs of the $X^2\Pi$ and $A^2\Sigma^+$ electronic states by the MRDCI approach. The active space of the MOs is prepared by the CASSCF method with the state averaging technique⁸ for one double occupied core MO and 7 electrons distributed over 9 active MOs. The total amount of configurations in MRDCI are about 6 millions for each of the X and A states. The aug-cc-pV5Z basis set is used at the O and H atoms. All calculations are carried out by GAMESS-US program package [20].

The results are shown in Figure 4.⁹ It is seen that the *ab initio* points perfectly follow the **Varandas-Voronin95** PEF. This result is very significant because the analytical results of Varandas and Voronin are confirmed by the first-principles calculation. From the point of view of the NIDL theory, this means that the analytical **Varandas-Voronin95** PEF is more suited for calculations of the overtone intensities than the point-wise **Brooke16** one since it has correct repulsive branch. Therefore, the **Varandas-Voronin95** potential is a good candidate for calculations of the overtone intensities. It should be noted that the **Brooke16** PEF is perfectly adjusted to describe the line positions. However, it cannot be excluded that the best description of the overtone intensities will be reached with a different PEF.

6. Conclusions

With use of the NIDL, we performed the analysis of the intensities calculated by Brooke *et al.* [8] and found that the intensities of the $\Delta v > 6$ transitions should not be trusted, in accord with our preliminary estimates [21].

The analysis of the OH data revealed one more limitation to the NIDL theory, in addition to the anomalies. Namely, the theory is not applicable to the satellite bands.

The effect of the small reduced mass, previously discovered in H₂ [18], causing the NIDL straight-line slope to be larger than the one associated with the repulsive branch of the potential, is demonstrated for OH as well. The same should be true of all the diatomic hydrides, HX.

Finally, we performed *ab initio* calculations of the OH repulsive branch and compared it with two OH potentials, one (point-wise, spline-interpolated) PEF of Brooke *et al.* [8] and the other (analytical) PEF due to Varandas and Voronin [17]. We found that the *ab initio* PEF closely follows the **Varandas-Voronin95** potential in the repulsive region, which is not surprising since the latter was specially constructed to correctly describe both asymptotic limits, in particular the united-atom limit so important in determination of the overtone intensities [2]. On the other hand, the **Brooke16** potential is perfectly suited to describe the line positions. Therefore, we dare to assume that, when selecting data for the spectroscopic databases like HITRAN, HITEMP, etc., different potentials can be used to calculate transition frequencies and transition intensities.

7. Additional remarks

In the NIDL theory, the transition matrix element is presented in the form of the product of the exponential factor, T_0 , and the prefactor, B_0 . The exponent of T_0 contains the difference of action integrals from zero to the inner turning points of the upper and lower rovibrational levels. T_0 depends solely on the repulsive branch of the potential and is responsible for the exponential decay of the overtone intensities presented graphically as a straight line in the NIDL coordinates whose slope is inversely proportional to the steepness of the repulsive branch. The prefactor depends on both the potential and the multipole moment function; it is on the order of the moment itself and can change sign between neighbouring rovibrational states, which results in anomalies, i.e. weak transitions, which fall down the NIDL line.

The NIDL theory is based on the WKB approximation, in which two lowest-orders terms in the BO parameter, $\kappa = (m_e/M)^{1/4}$, are retained. In view of small M , it well might be that the higher-order terms in κ contribute. We note, however, that the principal condition

for the WKB approximation is large action, $S/\hbar \gg 1$. Because of small M in the HX diatomics, the action is greatly reduced as compared to the heavier ones, ~ 20 vs ~ 1500 . Yet, it is large enough for WKB to fulfill with high accuracy. Even for H₂, the basic WKB approximation is almost exact, see Figure 3 in Ref. [18].

At the same time, the smaller action in light molecules has its specific effect on the rate of the intensity falloff with the overtone energy, the NIDL slope a . Namely, as mentioned above, the NIDL exponent is the difference of action integrals, which is also smaller in the HX molecules, hence a is significantly lower. In figures, $a = 4.3\text{--}6.8$ for HX and $a = 9.4$ for CO [22]. Owing to this slower decay of the intensities associated with the repulsive branch *via* the exponential factor in the TDM², the contribution of the prefactor to the decay rate becomes significant, as stated at the end of Section 4.

Another question associated with small M concerns the role of the mass-dependent adiabatic contribution to the BO potential and the non-adiabatic coupling. We remind that the BO PEF contains singularity (pole) at $r = 0$ due to Coulomb repulsion, which results in the NIDL. The adiabatic correction, which involves the second derivative of the wave function over r , is a smooth function having no singularity at short r , hence it cannot affect the repulsive branch of the potential and the NIDL. As for the non-adiabatic interaction, it also has no singularity at short r ; also, it couples the ground electronic state with the excited ones, which might in principle affect the wave functions, hence the intensities. However, there are larger terms in the Hamiltonian, *i.e.* the spin-orbit and rotational terms, that realise such couplings. The effect of such couplings on the NIDL will be considered in the forthcoming publication [16].

It is interesting to discuss Figure 4 in more detail. For calculations of the transition intensities in **Brooke16**, the RKR potential had to be interpolated between the outermost and innermost turning points and extrapolated beyond them. If the model PEF is not analytical, nonphysical saturation can appear at high-overtone transitions¹⁰; presumably, the slope of the repulsive branch can also change. However, the authors of Ref. [8] did not specify how the interpolation/extrapolation was done, especially which kind of the model function was used, therefore we cannot judge definitely why the repulsive branch so strongly declines from the *ab initio* calculations. The Referee calculated the derivatives of the Brooke *et al.* potential and found a jump in the third derivative at 0.7 Å, close to the inner classical turning point of the highest observed vibrational level $v = 13$ (0.697 Å). Hence, the function used in LEVEL [23] to model the PEF is not analytical, which results in the chaotic behaviour of the high-overtone intensities in

Figure 1 and probably could be responsible for the incorrect repulsive branch.

On the contrary, the Varandas-Voronin potential is strictly analytical and, moreover, was constructed so as to reproduce the asymptotic limits of short and long r ; therefore, it is more suitable for calculating the intensities up to the highest overtones. However, it is crude with respect to the transition frequencies because it uses old RKR points. We do not propose to use this PEF for calculating the intensities, it is cited merely as a good example of an analytic model to be used in future work. Namely, a temptation arises to refine the Varandas-Voronin PEF by using the new RKR points of **Brooke16** and Mitev *et al.* [24]. However, this is not a simple task, which is beyond the scope of the present paper. There well may be that different potentials should be used for precise calculations of frequencies and intensities. In the current work [16], we follow our method that uses analytical model functions with parameters determined by least-squares fitting to the line positions and other experimental and theoretical data without using the RKR tabulated potentials.

Notes

1. Actually, even $\nu = 0$ and 1 can be treated quasi-classically because the NIDL formalism considers the wave functions in the complex plane far enough from the turning points where the quasi-classical behaviour is assured, but we leave aside this issue since it is beyond the scope of the present paper.
2. This important notion means that any model theoretical PEF must not have any other singularities affecting the TDMs.
3. For brevity, we will call the product, $A\lambda^3 \propto \text{TDM}^2$, the intensity.
4. But see below, Section 4.
5. See, however, Section 4; the DMF is also responsible for the anomalies, which drop off the NIDL line.
6. The NIDL theory was developed for purely vibrational transitions, therefore only low J are in order to consider to minimise the effect of rotation.
7. It is difficult to exclude all the anomalies. A subset of the anomalies seemingly following its own NIDL with the same slope and a large negative const in Equation (2) actually corresponds to a single $\nu - \nu_1$ anomaly.
8. Averaging over two Π and one Σ states.
9. The *ab initio* data for the repulsive branch of the $X^2\Pi$ state are given in Supplementary material.
10. The molecular hydrogen is an exception: using splines, which have jumps in derivatives at every grid point, does not deteriorate the intensities owing to high-precision *ab initio* calculations and very dense grid of interatomic separations [18].

Acknowledgments

We are grateful to the Referee for calculations mentioned in Section 7 and other helpful comments.

Disclosure statement

No potential conflict of interest was reported by the author(s).

Funding

This work was performed under state task, Ministry of Science and Education, Russian Federation [state registration number 124013000760-0].

ORCID

Emile S. Medvedev  <http://orcid.org/0000-0002-4415-6926>

Aleksander Yu. Ermilov  <http://orcid.org/0009-0007-2804-9120>

Vladimir G. Ushakov  <http://orcid.org/0000-0002-4070-0568>

References

- [1] A.Y. Ermilov, E.S. Medvedev and A.V. Nemukhin, *Opt. Spectrosc.* **69**, 554–557 (1990) [*Opt. Spectrosc.* **69**, 331 (1990)].
- [2] E.S. Medvedev, *J. Chem. Phys.* **137**, 174307 (2012). [2012 Editors' Choice]. doi:10.1063/1.4761930
- [3] G. Li, I.E. Gordon, L.S. Rothman, Y. Tan, S.-M. Hu, S. Kassi, A. Campargue and E.S. Medvedev, *Astrophys. J. Suppl. Ser.* **216**, 15 (2015). doi:10.1088/0067-0049/216/1/15
- [4] V.G. Ushakov, M. Semenov, S.N. Yurchenko, A.Y. Ermilov and E.S. Medvedev, *J. Molec. Spectrosc.* **395**, 111804 (2023). doi:10.1016/j.jms.2023.111804
- [5] V.I. Krassovsky, N.N. Shefov and V.I. Yarin, *J. Atmos. Terr. Phys.* **21**, 46–53 (1961). doi:10.1016/0021-9169(61)90190-8
- [6] P.C. Cosby and T.G. Slanger, *Can. J. Phys.* **85**, 77–99 (2007). doi:10.1139/p06-088
- [7] E.S. Medvedev, *Spectrosc. Lett.* **18**, 447–461 (1985). doi:10.1080/00387018508062244
- [8] J.S.A. Brooke, P.F. Bernath, C.M. Western, C. Sneden, M. Afşar, G. Li and I.E. Gordon, *J. Quant. Spectrosc. Radiat. Transfer* **168**, 142–157 (2016). doi:10.1016/j.jqsrt.2015.07.021
- [9] S. Noll, H. Winkler, O. Goussev and B. Proxauf, *Atmos. Chem. Phys.* **20**, 5269–5292 (2020). doi:10.5194/acp-20-5269-2020
- [10] I.E. Gordon, L.S. Rothman, R.J. Hargreaves, R. Hashemi, E.V. Karlovets, F.M. Skinner, E.K. Conway, C. Hill, R.V. Kochanov, Y. Tan, P. Wcisło, A.A. Finenko, K. Nelson, P.F. Bernath, M. Birk, V. Boudon, A. Campargue, K.V. Chance, A. Coustenis, B.J. Drouin, J. Flaud, R.R. Gamache, J.T. Hodges, D. Jacquemart, E.J. Mlawer, A.V. Nikitin, V.I. Perevalov, M. Rotger, J. Tennyson, G.C. Toon, H. Tran, V.G. Tyuterev, E.M. Adkins, A. Baker, A. Barbe, E. Canè, A.G. Császár, A. Dudaryonok, O. Egorov, A.J. Fleisher, H. Fleurbaey, A. Foltynowicz, T. Furtenbacher, J.J. Harrison, J. Hartmann, V. Horneman, X. Huang, T. Karman, J. Karns, S. Kassi, I. Kleiner, V. Kofman, F. Kwabia-Tchana, N.N. Lavrentieva, T.J. Lee, D.A. Long, A.A. Lukashovskaya, O.M. Lyulin, V.Y. Makhnev, W. Matt, S.T. Massie, M. Melosso, S.N. Mikhailenko, D. Mondelain, H.S.P. Müller, O.V. Naumenko, A. Perrin,

- O.L. Polyansky, E. Raddaoui, P.L. Raston, Z.D. Reed, M. Rey, C. Richard, R. Tóbiás, I. Sadiék, D.W. Schwenke, E. Starikova, K. Sung, F. Tamassia, S.A. Tashkun, J.V. Auwera, I.A. Vasilenko, A.A. Vigin, G.L. Villanueva, B. Vispoel, G. Wagner, A. Yachmenev and S.N. Yurchenko, *J. Quant. Spectrosc. Rad. Transfer* **277**, 107949 (2022). doi:10.1016/j.jqsrt.2021.107949
- [11] E.S. Medvedev and V.I. Osherov, *Radiationless Transitions in Polyatomic Molecules*, Springer Series in Chemical Physics, 57 vols. (Springer-Verlag, Berlin, 1995).
- [12] L.D. Landau and E.M. Lifshitz, *Quantum Mechanics: Non-Relativistic Theory*, 3rd ed. (Pergamon, Oxford, 1977).
- [13] A.F. Ferguson and D. Parkinson, *Planet. Space Sci.* **11**, 149–159 (1963). doi:10.1016/0032-0633(63)90136-3
- [14] F.H. Mies, *J. Mol. Spectrosc.* **53**, 150–188 (1974). doi:10.1016/0022-2852(74)90125-8
- [15] D.D. Nelson Jr., A. Schiffman, D.J. Nesbitt and D.J. Yaron, *J. Chem. Phys.* **90**, 5443–5454 (1989). doi:10.1063/1.456450
- [16] V.G. Ushakov, A.Y. Ermilov and E.S. Medvedev, Three-states model for calculating the X-X rovibrational transition intensities in hydroxyl radical, in preparation (2024).
- [17] A.J.C. Varandas and A.I. Voronin, *Chem. Phys.* **194**, 91–100 (1995). doi:10.1016/0301-0104(94)00424-9
- [18] V.G. Ushakov, S.A. Balashev and E.S. Medvedev, *J. Molec. Spectrosc.* **399**, 111863 (2024). doi:10.1016/j.jms.2023.111863
- [19] E.S. Medvedev and V.G. Ushakov, *J. Quant. Spectrosc. Radiat. Transfer* **288**, 108255 (2022). doi:10.1016/j.jqsrt.2022.108255
- [20] G.M.J. Barca, C. Bertoni, L. Carrington, D. Datta, N. De Silva, J.E. Deustua, D.G. Fedorov, J.R. Gour, A.O. Gunina, E. Guidez, T. Harville, S. Irle, J. Ivanic, K. Kowalski, S.S. Leang, H. Li, W. Li, J.J. Lutz, I. Magoulas, J. Mato, V. Mironov, H. Nakata, B.Q. Pham, P. Piecuch, D. Poole, S.R. Pruitt, A.P. Rendell, L.B. Roskop, K. Ruedenberg, T. Sattasathuchana, M.W. Schmidt, J. Shen, L. Slipchenko, M. Sosonkina, V. Sundriyal, A. Tiwari, J.L. Galvez Vallejo, B. Westheimer, M. Wloch, P. Xu, F. Zahariev and M.S. Gordon, *J. Chem. Phys.* **152**, 154102 (2020). doi:10.1063/5.0005188
- [21] E.S. Medvedev and V.G. Ushakov, *Opt. Spectrosc.* **130**, 1077–1084 (2022). doi:10.21883/EOS.2022.09.54822.3428-22
- [22] E.S. Medvedev, *J. Mol. Spectrosc.* **114** (1), 1–12 (1985). doi:10.1016/0022-2852(85)90330-3
- [23] R.J. Le Roy, *J. Quant. Spectrosc. Rad. Transfer* **186**, 167–178 (2017). doi:10.1016/j.jqsrt.2016.05.028
- [24] G.B. Mitev, J. Tennyson and S.N. Yurchenko, *J. Chem. Phys.* **160**, 144110 (2024). doi:10.1063/5.0198241